A NUMERICAL CODE FOR THE PREDICTION OF BED-LOAD AND OF SURFACE INSTABILITIES ON A GRANULAR BED SHEARED BY A TURBULENT BOUNDARY-LAYER

Erick de Moraes Franklin, erick@unifei.edu.br
Instituto de Engenharia Mecânica – Universidade Federal de Itajubá

Abstract. *The transport of solid particles entrained by a fluid flow is frequently found in nature and in industrial environments. If the shear stresses exerted by the fluid on the granular bed are bounded to some limits, a mobile granular layer takes place in which the grains stay in contact with the fixed bed, known as bed-load. When the fluid is a liquid, the thickness of this mobile layer is a few grain diameters. Under these conditions, an initially flat granular bed may be unstable, giving rise to ripples and dunes. These forms can be observed in nature, as for instance the sand dunes seen in deserts, but also in industrial applications, such as the dunes appearing in petroleum pipelines conveying sand. This communication presents a mathematical model for the transport of grains as bed-load by a turbulent boundary-layer, when the fluid is a liquid. The model is simple, but able to capture the pertinent physics involved, such as the growing of instabilities on the bed surface. Some simulations are presented and confronted to the linear stability analysis of granular beds under turbulent boundary-layers.*

Keywords*: Mathematical modeling, turbulent boundary-layer, bed-load, instability*

1. INTRODUCTION

The transport of solid particles entrained by a fluid flow is frequently found in nature and in industry. It is present, for example, in the erosion of river banks, in the displacement of desert dunes and in hydrocarbon pipelines conveying sand. When shear stresses exerted by the fluid flow on the granular bed are able to move some grains, but are relatively small compared to their weight, the flow is not able to transport grains as a suspension. Instead, a mobile layer of grains known as bed-load takes place in which the grains stay in contact with the fixed part of the granular bed. The thickness of this mobile layer is a few grain diameters (Bagnold, 1941; Raudkivi, 1976).

An initially flat granular bed may become unstable and give rise to bedforms when submitted to a fluid flow. These forms, initially two-dimensional, may grow and generate patterns such as ripples or dunes. In nature, some examples affecting human activities are the aeolian and the aquatic dunes. The aquatic ripples and dunes observed on the bed of some rivers create a supplementary friction between the bed and the water, affecting the water depth and being related to flood problems. In cases where their size is comparable to the water depth, water flows can experiment local depth variations, seriously affecting navigation (Engelund and Fredsoe, 1982). In industry, examples are mostly related to closed-conduit flows conveying grains, such as hydrocarbon pipelines conveying sand. In such cases, the bedforms generate supplementary pressure loss, but also pressure and flow rate transients (Kuru et al., 1995; Franklin, 2008).

The stability of a granular bed is given by the balance between the local erosion and deposition of grains. If there is erosion at the crests of the granular bed, the amplitude of initial bed undulations decreases and the bed is stable. On the contrary, the bed is unstable. If there is neither erosion nor deposition at the crests, there is neutral stability. The regions of erosion and deposition can be found from the mass conservation of grains. The mass conservation implies that there is erosion in regions where the gradient of the flow rate of grains is positive and deposition where it is negative, so that the phase lag between the flow rate of grains and the bedform is a stability criterion. If the maximum of the flow rate of grains is upstream a crest, there must be deposition at the crest and the bed is unstable, otherwise the bed is stable. To answer the stability question, the mechanisms creating a phase lag between the flow rate of grains and the shape of the granular bed need to be known.

In order to understand the problem, many works on the stability of granular beds sheared by a fluid were made in the last decades (Kennedy, 1963; Reynolds, 1964; Engelund, 1970; Richards, 1980; Elbelrhiti et al., 2005; Claudin and Andreotti, 2006; for instance). A remarkable description of this approach can be found in Engelund and Fredsoe (1982).

In a recent article (Franklin, 2010), the mechanisms of this instability were explained and a linear stability analysis was presented, in the specific case of granular beds sheared by turbulent boundary-layers of liquids, without free surface effects. It was seen that the basic mechanisms are three: the fluid flow perturbation by the shape of the bed, which is known to be the unstable mechanism (Jackson et al., 1975; Hunt et al., 1988; Weng et al., 1991), the relaxation effects related to the transport of grains and the gravity effects, which are the stable mechanisms (Valance and Langlois (2005) and Charru (2006) in the case of viscous flows, Franklin (2010) in the case of turbulent flows). The linear stability analysis of Franklin (2010) showed that the length-scale of the initial bedforms varies with both the grains diameter and the fluid flow conditions.

Franklin (2011) presented a nonlinear stability analysis in the same scope of Franklin (2010). The approach used was the weakly nonlinear analysis (Landau and Lifchitz, 1994; Schmid and Henningson, 2001; Drazin and Reid, 2004; Charru, 2007), useful whenever a dominant mode can be proved to exist. This means that the modes resonating with

this dominant one will grow much faster than the others, which can be neglected. The analysis is then made on a bounded number of modes. Franklin (2011) showed that after the initial exponential growth (linear phase), the granular bed instabilities saturate, i.e., they attenuate their growth rate and maintain the same wavelength.

In both articles, Franklin (2010) and Franklin (2011), the results of the analyses were compared to some experimental data concerning ripples in closed-conduit flows (which is a case where the free surface is absent). In particular, the dependence of the bedform wavelength on the fluid flow conditions and the saturation of the bedform amplitude were confirmed by experimental results.

Bed-load numerical simulations are another approach in the effort to understand the instabilities on granular beds. The main problem is then the modeling of the granular media: it is a discrete media for which a lagrangian description is not practical given the large number of discrete elements. To solve this problem, it is usual to employ semi-empirical relations for the bed-load flow rate, such as that of Bagnold (1941) and that of Meyer-Peter and Mueller (1948).

Amongst the numerical models for the case of turbulent boundary-layers, there are Kroy et al. (2002a), Kroy et al. (2002b) and Hersen (2004). These models were all conceived for turbulent gas flows (aeolian case), and are based on four basic equations: (i) the shear stress caused by the fluid flow on the bed surface; (ii) a semi-empirical equation for the bed-load; (iii) an equation accounting for the relaxation between the fluid flow and the granular flow; and (iv) the mass conservation of the grains.

In their model, because the relations for bed-load are based on the shear stress on the bed, Kroy et al. (2002a) and Kroy et al. (2002b) proposed the direct use of an equation for the shear stress on the bed, instead of computing the fluid flow in the entire domain. The shear stress caused by the fluid flow on the bed can be obtained by Perturbations Methods, such as, for example, Jackson et al. (1975), Hunt et al. (1988) and Weng et al. (1991) for the case of turbulent boundary-layers. Kroy et al. (2002a) and Kroy et al. (2002b) simplified the results of Jackson et al. (1975), Hunt et al. (1988) and Weng et al. (1991) and obtained an expression containing only the dominant physical effects of the perturbation. Concerning the bed-load flow rate, they employed an equation derived from the aeolian bed-load model of Sauermann et al. (2001), whose constants were adjusted from experimental data (so that the model is semi-empirical). The employed equation accounting for the relaxation between granular and fluid flow rates was also from Sauermann et al. (2001). The model was then implemented in a numerical code and some simulations were performed. From different initial conditions, the model was able to show the evolution from the initial bump to dunes, including the three-dimensional crescent-shape dunes (barchan dunes) in the case of three-dimensional simulations.

The model presented in Hersen (2004) is based on the same equations of Kroy et al. (2002a) and Kroy et al. (2002b). The main difference in Hersen (2004) is that the focus of the performed simulations is the understanding of the formation of barchan dunes.

This communication presents a mathematical model for the bed-load transport of grains by a turbulent boundary-layer when the fluid is a liquid. The model is kept as simple as possible, but it is able to capture the pertinent physics involved, such as the growing of instabilities on the bed surface. Different from Kroy et al. (2002a), Kroy et al. (2002b) and Hersen (2004), that were interested in the evolution of bed-forms towards a stationary solution (dunes), the present model focus on the very early stages of the bed instabilities. Another difference is that the model is applied to liquids, for which some bed-load characteristics are different from the aeolian case. Its implementation in a numerical code is discussed and some simulations are presented and confronted to the linear stability analysis of Franklin (2010).

The next section discusses the involved physics and presents the equations composing the model. The following sections describe the numerical implementation of the model in a computational code, and the main results from the numerical simulations. They are followed by the conclusion section.

2. MATHEMATICAL MODELING OF THE BED-LOAD TRANSPORT

The present model follows the lines of Kroy et al. (2002a), Kroy et al. (2002b) and Hersen (2004), and is also based on the following four equations: (i) the shear stress caused by the fluid flow on the bed surface; (ii) a semi-empirical equation for the bed-load transport; (iii) an equation accounting for the relaxation between the fluid flow and the granular flow; and (iv) the mass conservation of the granular matter. However, those equations are worked differently here, mainly with respect to relaxation effects, and to the inclusion of gravity effects. Different from Kroy et al. (2002a), Kroy et al. (2002b) and Hersen (2004), the present model is applicable to turbulent liquid flows, and is focused in the early stages of the bed instabilities.

As the interest here is in the first stages of the bed instabilities, the model is two-dimensional. This is justified by the Squire's Theorem, which states that the most unstable modes in parallel flows are two-dimensional (Schmid and Henningson, 2001; Drazin and Reid, 2004; Charru, 2006). The physical concepts and the equations employed in the model are presented next.

2.1. Shear stress on the bed

The perturbation of a turbulent boundary-layer by a hill with small aspect ratio was analytically found by Jackson and Hunt (1975) and by Hunt et al. (1988). Their results were later applied to forms with higher aspect ratio by Weng et

al. (1991). Jackson and Hunt (1975), Hunt et al. (1988) and Weng et al. (1991) found that the perturbed shear stress is shifted upstream the dune crest. Kroy et al. (2002a) and Kroy et al. (2002b) simplified the results of Weng et al. (1991) and obtained an expression containing only the dominant physical effects of this perturbation, making clear the reasons for this upstream shift. For a two-dimensional hill with a height $h(x)$, a surface rugosity y_0 and a length $2L$ between the half-heights (total length ≈ $4L$), they showed that the perturbation of the longitudinal shear stress, in dimensionless form and in the Fourier space, is

$$\hat{\tau}_k = AF\{h\}(|k| + iBk) \tag{1}$$

where $k = 2\pi\lambda^{-1}$ is the wave-number (λ is the wavelength), i is the imaginary number, the subscript k is related to the Fourier space, F is the Fourier transform operator, x is the longitudinal direction and A and B are considered as constants, as they vary with the logarithm of L/y_0. Equation (1) was obtained for $H/L < 0.05$, but Carruthers and Hunt (1990) showed that reasonable results are obtained when Eq. (1) is applied for slopes up to $H/L = 0.3$. The fluid flow over the bed can be written as a basic flow, unperturbed, plus a flow perturbation. The shear stress on the surface of the bed can then be written, in the real space, as

$$\tau = \tau_0\left(1 + F^{-1}\{\hat{\tau}_k\}\right) \tag{2}$$

where τ_0 is the shear stress caused by the basic flow on a flat bed (basic state) and F^{-1} is the inverse Fourier operator.

The shear stress caused by the fluid flow on the bed surface can be obtained directly from Eqs. (1) and (2). The great advantage of this method is that there is no need to compute the fluid flow in regions far from the surface, as it would be necessary with, for example, a RANS (Reynolds Average Navier-Stokes) method.

2.2. Flow rate of grains in the basic state

In a steady state regime, and without spatial variations, the fluid flow and the flow rate of grains are in equilibrium (basic state). The equilibrium flow rate of grains is known as "saturated flow rate of grains". However, given the discrete nature of granular matter, there are many different formulations (and a lack of consensus) for the flow rate of grains. The existing formulas are semi-empirical, and the one employed here is that of Meyer-Peter and Mueller (1948)

$$\frac{q_{sat}}{\sqrt{(S-1)gd^3}} = 8(\theta - \theta_t)^{3/2} \tag{3}$$

where q_{sat} is the volumetric flow rate of grains by unit of width, S is the ratio between the grains specific mass ρ_p and the fluid specific mass ρ, g is the acceleration of gravity, d is the mean grain diameter, θ is the Shields parameter

$$\theta = \frac{\tau}{(\rho_p - \rho)gd} \tag{4}$$

and θ_t is the threshold Shields parameter (Buffington and Montgomery, 1997).

2.3. Relaxation between the flow rate of grains and the fluid flow rate

In the case of a fluid flow over an undulated bed, the shear stress caused by the fluid on the bed is a function of the position. The flow rate of grains will lag some distance (or time) with respect to the fluid flow, being then a stable mechanism. This distance is a characteristic length usually called "saturation length", L_{sat}. A simplified expression taking into account this relaxation effect can be obtained from the erosion-deposition model of Charru et al. (2004)

$$\partial_x q = \frac{q_{sat} - q}{L_{sat}} \tag{5}$$

Kroy et al. (2002a), Kroy et al. (2002b) and Hersen (2004) considered that the saturation length has an inertial origin, and is proportional to the traveling distance of individual grains, given by $L_{drag} = d\ \rho_p/\rho$. According to this expression, L_{drag} is an inertial length-scale obtained when the density of the granular material is many times larger than the density of the fluid, $\rho_p >> \rho$. It is then pertinent when the fluid is a gas. When the fluid is a liquid, however, $\rho_p \approx \rho$ and it was argued by Charru (2006) and by Franklin (2010) that this length-scale can no longer be applied. Instead, a relaxation length based on the deposition of an individual grain must be used, L_d

$$L_{sat} = C_{sat} L_d = C_{sat} d\left(u_{*0} / U_S \right) \tag{6}$$

where u_{*0} is the shear velocity of the basic flow, defined by $\tau = \rho u_{*0}^2$, U_s is the grain settling velocity and C_{sat} is an adjustable constant. For a large range of settling Reynolds numbers ($Re_S = \rho U_S d/\mu$), the settling velocity U_s may be evaluated as

$$U_S = \left[\frac{4}{3} \frac{1}{C_D} gd \left(\frac{\rho_p - \rho}{\rho} \right) \right]^{1/2} \tag{7}$$

where C_D is the drag coefficient, that may be evaluated by the Schiller-Neuman correlation when $Re_S < 800$ (Clift et al., 1978).

2.4. Mass conservation of grains

The two-dimensional mass conservation applied to the grains can be written as

$$\partial_t h + \partial_x q = 0 \tag{8}$$

where the porosity of the granular material was omitted for simplicity because it is constant in this problem.

2.5. Gravity effects

As discussed in Franklin (2010), gravity weakens the transport of grains over positive slopes (upstream the crests) and facilitates it over negative slopes (downstream the crests), being inversely proportional to the slope of the bed. It can then be incorporated in the constant B of the shear stress perturbation (Eq. 1).

2.6. Model structure

Computations from the model are relatively fast and easy. First, there is no need to compute the fluid flow in the entire domain because the model needs only the shear stress on the bed, whose analytical solutions obtained by the Perturbation Methods are known. Second, two of the four basic equations have analytical solutions, so that they can be computed directly in sequence (they are uncoupled). The other two equations are first order and uncoupled, they may then be numerically computed with simple schemes. The computations may be done directly and there is no need for iterations. Given an upstream condition (the boundary condition, which is in fact the basic state) and an initial bed (initial condition), the solution scheme (in two-dimensions) is a loop containing the following steps:

(i) Computation of the shear stress $\tau(x)$ on the bed employing Eqs. (1) and (2);
(ii) Computation of the flow rate of grains in the basic state $q_{sat}(x)$ by Eq. (3);
(iii) Computation of the actual flow rate of grains $q(x)$ by Eq. (5);
(iv) Computation of the bed $h(x)$ at the new time step by Eq.(8) (this is an integration in time);

These steps must be done until the required final time (or total number of iterations) is achieved.

3. NUMERICAL IMPLEMENTATION

The model was implemented in a numerical code, following the structure given in sub-section 2.6. The code structure is given below. An explanation of some of the numerical steps follows.

1. Entry:
    a. Fluid and grains properties
    b. Boundary condition (u_{*0})
    c. Initial condition (initial $h(x)$)
    d. Numerical parameters
    e. Computation of L_{sat} by Eq. (6)
2. Loop (until the desired number of iterations, or the total time, is achieved):
    a. Fourier transform of $h(x)$
    b. Computation of $\hat{\tau}_k$ by Eq. (1)
    c. Inverse Fourier transform of $\hat{\tau}_k$
    d. Computation of τ by Eq.(2)
    e. Computation of $q_{sat}(x)$ by Eq. (3);

f. Computation of *q(x)* by the numerical solution of Eq. (5);
g. Computation of the new values of *h(x)* by the numerical solution of Eq. (8)
h. Storage of the data at the desired time instants

3. Post-processing
   a. Computation of the bedform growth rate
   b. Computation of the bedform celerity
   c. Plot of the desired curves

A brief explanation of some of the numerical steps is given below.

- Fluid and grain properties (1.a): these concern the specific masses of the liquid and of the grains, the dynamic viscosity of the liquid, the mean diameter of the grains and the threshold velocity for the grains mobilization.
- Boundary condition (1.b): is the condition far upstream the initial bedform, corresponding then to the basic state because the flow in this region is unperturbed. In the code, the entry is the unperturbed shear velocity $u_{*0} = \sqrt{\tau_0 / \rho}$.
- Initial condition (1.c): it is the initial form of the bed *h(x).*
- Numerical parameters (1.d): they correspond to the numerical constants necessary to the code functioning. They are: the spatial resolution Δx, the time step Δt, the total number of iterations N and the numerical scheme to be employed in the numerical solution of Eq. (8).
- Computation of L_{sat} (1.e): L_{sat} is evaluated by Eq. (6) employing the unperturbed shear velocity u_{*0}.
- Computation of $\tau(x)$ (2.a to 2.d): it is divided in four steps. First, a Fast Fourier Transform (FFT) operation is made on h. Then, $\hat{\tau}_k$ is evaluated by Eq. (1) and an Inverse Fast Fourier Transform (IFFT) operation is made on $\hat{\tau}_k$. Finally, $\tau(x)$ is evaluated by Eq. (2).
- Computation of $q_{sat}(x)$ (2.e): the Shields parameter is evaluated by Eq. (4) and $q_{sat}(x)$ is evaluated by Eq. (3).
- Computation of *q(x)* (2.f): *q(x)* is evaluated by the numerical integration of Eq. (5). For this integration an Upwind scheme is employed, with the boundary condition $q(x=0) = q_{sat}(x=0)$.
- Computation of *h(x)* for the new time step (2.g): *h(x)* is evaluated by the numerical solution of Eq. (8). As *q(x)* and $q_{sat}(x)$ are already known, an explicit numerical scheme can be simply employed to determine *h(x)* in the new time step. In the code, one can choose between four schemes that were implemented: LAX + FTCS, Upwind + LAX, Upwind + First Order Euler, FTCS + First Order Euler. Due to the very small phase shifts between *q(x)* and *h(x)* in some cases, the First Order Euler schemes work better than the LAX schemes, as explained in what follows.
- Storage of the data (2.i): at the desired time steps, *q(x)* and *h(x)* are stored.
- Computation of the bedform growth rate and of the bedform celerity (3.a and 3.b): the growth rate σ and the bedform celerity c are evaluated from the transversal and the longitudinal displacement velocities of the bedform crest, respectively. Those velocities are evaluated by fitting the displacements as linear functions of the time.

For all the simulations presented here the initial bedform was a Gaussian Function

$$h(x) = H\, e^{-\frac{(x-\mu)^2}{2s_d^2}} \tag{9}$$

where H is the initial amplitude (crest), μ is the mean and s_d is the standard deviation. This form has the advantage of tending to zero when the domain is large enough, meaning that the basic state is expected to exist on the boundaries of the domain. Another advantage is that it can be easily adjusted to different sizes, positions and aspect rations by varying H, s_d and μ. In order to be coherent with Jackson and Hunt (1975), Hunt et al. (1988) and Weng et al. (1991), it is considered here that $L=4s_d$ so that the total length is approximately $4s_d$.

The simulations presented here employed the scheme Upwind + First Order Euler for the numerical solution of Eq. (8), which gave better results. Given the small phase shifts between *q(x)* and *h(x)* in some cases, the schemes based on LAX become more dependent on the spatial resolution because they employ a spatial average on the preceding time steps. This phase shift is the responsible for the stability or the instability of the bedform (Franklin, 2010). The use of an explicit scheme for the numerical solution of Eq. (8) means that the Courant condition must be verified. This was assured for all the simulations.

4. MAIN RESULTS

Simulations were performed employing the numerical code described in section 3, and the preliminary results are presented here. For these simulations, the aspect ratio of the initial bedform was fixed, and the shear velocity was varied. Gravity (slope) effects and grains diameter are not discussed in this communication. The bedform evolution was

then computed and its growth rate and celerity were evaluated. Table 1 presents a summary of the entry parameters and of the main results.

Figure 1 shows three examples of bedform development predicted by the numerical code. The initial form, shown in dashed line (blue) was a Gaussian function with $s_d = 0.1m$ and aspect ratio $H/(4s_d) = 0.1$. For the simulation presented in Fig. 1, the total number of iterations was 10^5 with a time step $\Delta t = 10^{-5}s$, corresponding then to a total time of $1s$. The total domain in the x direction was $2m$ and it was discretized in intervals of $\Delta x = 10^{-3}m$. The saturation adjustable constant is $C_{sat}=1$. Figure 1.a corresponds to $u_{*0} = 0.04$ m/s, Fig 1.b corresponds to $u_{*0} = 0.08$ m/s and Fig. 1.c corresponds to $u_{*0} = 0.16$ m/s.

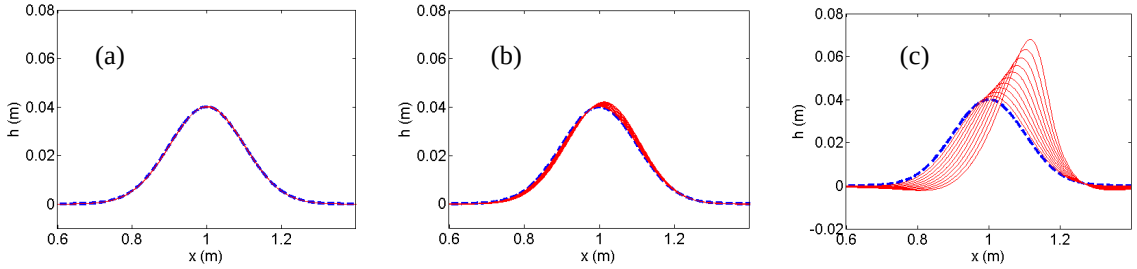

Figure 1. Evolution of an initial gaussian bedform, with $s_d = 0.1m$ and aspect ratio $H/(4s_d) = 0.1$. The dashed line is the initial form and the continuous lines correspond to the bedform at posterior times. The total time for this simulation was 1 s. The saturation adjustable constant is $C_{sat}=1$. (a) corresponds to $u_{*0} = 0.04$ m/s, (b) corresponds to $u_{*0} = 0.08$ m/s and (c) corresponds to $u_{*0} = 0.16$ m/s.

From Figs. 1.b and 1.c it is clear that the simulated cases are unstable, with the bedform growing as the time increases, while the form is displaced to the right, showing a positive celerity. The same occurs in Fig. 1.a, however the time-scale is too large (slow growth rate) to be clear in the figure. The slope of the upwind face (upstream the crest) decreases, while the slope of the lee face (downstream the crest) increases. This indicates that the initial gaussian bedform tends to a transverse ripple form, which has an upstream face of small slope, and a high slope lee face (in fact an avalanche slope). This is exactly what is verified experimentally (Franklin, 2010; Franklin, 2011), so that the model is able to qualitatively predict the bedform evolution in the early stages of the instability (or stability). Also from Fig. 1, it is clear that the growth rate and the celerity of the bedforms increase with the shear velocity of the basic flow.

Table 1. Bedform celerity c and growth rate σ for different values of the saturation constant C_{sat} and differnt shear velocities of the basic flow u_{*0}. Δx is the spatial intervals (resolution), Δt is the time step, N is the total number of iterations and X is the longitudinal length of the computation domain. $s_d = 0.1m$ and aspect ratio $H/(4s_d) = 0.1$.

Δx (m)	Δt (s)	N	X (m)	Csat	U*0 (m/s)	C (m/s)	σ (1/s)
1E-03	1E-05	1E+05	2	1	0.04	0.0016	0.00068
1E-03	1E-05	1E+05	2	1	0.08	0.0130	0.00540
1E-03	1E-05	1E+05	2	1	0.16	0.1155	0.04210
1E-03	1E-05	1E+05	2	10	0.04	0.0017	0.00059
1E-03	1E-05	1E+05	2	10	0.08	0.0139	0.00450
1E-03	1E-05	1E+05	2	10	0.16	0.1134	0.02800
1E-03	1E-05	1E+05	2	25	0.04	0.0019	0.00051
1E-03	1E-05	1E+05	2	25	0.08	0.0138	0.00300
1E-03	1E-05	1E+05	2	25	0.16	0.1021	0.00880
1E-03	1E-05	1E+05	2	50	0.04	0.0019	0.00037
1E-03	1E-05	1E+05	2	50	0.08	0.0126	0.00110
1E-03	1E-05	1E+05	2	50	0.16	0.0805	-0.00840

In order to obtain more quantitative results to be compared to analytical stability analyses, the growth rate and the celerity of the bedform were computed. For the present simulations, the growth rate σ was evaluated as the transversal displacement velocity of the crest divided by the total length, and the bedform celerity c was evaluated as the longitudinal displacement velocity of the crest. These results are summarized in Tab. 1.

Table 1 shows the bedform celerity c and the growth rate σ obtained in simulations where the adjustable constant C_{sat} and the shear velocity of the basic flow u_{*0} were varied, but an initial wavelength was imposed.

From Tab.1, when $C_{sat}=1$ or $C_{sat}=10$, variations of the shear velocity of the basic flow u_{*0} by a factor m implies variations in both the bedform celerity c and in the growth rate σ by a factor m^3. The variation of c and of σ as u_{*0}^3 indicates that c and σ vary directly with the saturated flow rate of grains in the basic state (Franklin, 2010): the effect of the saturation length L_{sat} is too weak to cause effects in the celerity or in the growth rate. In fact, as discussed in Franklin (2010), the modulation of the length-scale, of the celerity and of the growth rate depend on the phase shift

between the fluid flow and the bed morphology (unstable effect) and on the phase shift between the bed-load flow rate and the fluid flow (stable effect). When $C_{sat}=1$ or $C_{sat}=10$, the phase shift between the bed-load flow rate and the fluid flow (stable effect), although it exists, is too small (many times smaller than the phase shift between the fluid flow and the bed morphology) to affect c and σ, so that they vary only with the saturated flow rate of grains (in the basic state).

If the value of C_{sat} is increased to $C_{sat}=25$ or $C_{sat}=50$, the phase shift between the bed-load flow rate and the fluid flow (stable effect) is increased and both the celerity and the growth rate show variations that are lower than u_{*0}^3, indicating that the relaxation effects are present. For the case $C_{sat}=50$ and $u_{*0}=0.16$ m/s, the growth rates are negative, indicating strong relaxation effects and stability. Figure 2 shows the curves of $h(x)$ (dotted blue line), $q_s(x)$ (dashed line) and $q_b(x)$ (continuous red line) normalized by their maxima. In this figure, $q_b=q$. Figure 2.a corresponds to $u_{*0}=0.04$ m/s and $C_{sat}=1$, Fig 2.b corresponds to $u_{*0}=0.04$ m/s and $C_{sat}=25$ and Fig. 2.c corresponds to $u_{*0}=0.16$ m/s and $C_{sat}=50$. All the other parameters are the same as in Fig. 1.

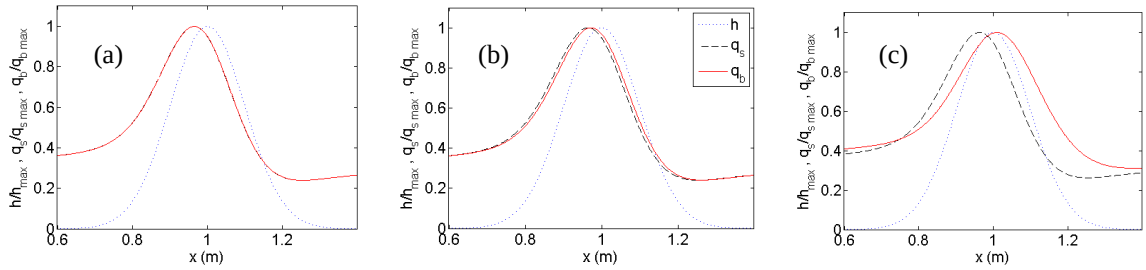

Figure 2. Curves of $h(x)$ (dotted blue line), $q_s(x)$ (dashed line) and $q_b(x)$ (continuous red line) normalized by their maxima. In this figure, $q_b=q$. (a) corresponds to $u_{*0}=0.04$ m/s and $C_{sat}=1$, (b) corresponds to $u_{*0}=0.04$ m/s and $C_{sat}=25$ and (c) corresponds to $u_{*0}=0.16$ m/s and $C_{sat}=50$.

From Fig.2a, it is clear that the phase shift between $q_b=q$ and q_{sat} is neglectful when $u_{*0}=0.04$ m/s and $C_{sat}=1$: it is many times smaller than the phase shift between q_b (in phase with the fluid flow) and the bed morphology. This explains the absence of effects related to the relaxation of the bed-load in the cases where $C_{sat}=1$. On the other hand, Figs. 2.b shows that the phase shift between q_b and q_{sat} is noticeable when $u_{*0}=0.04$ m/s and $C_{sat}=25$, so that the effects of relaxation are expected to exist. Finally, Fig. 2.c shows that a strong phase shift is produced between q_b and q_{sat} when $u_{*0}=0.16$ m/s and $C_{sat}=50$. This phase shift is so large that the maximum of $q_b(x)$ occurs downstream the crest of the bedform, and the bed tends to flatten: the granular bed is stable (Franklin, 2010).

Figure 3 shows the bedform development predicted by the numerical code when $C_{sat}=50$. The initial form, shown in dashed line (blue) was a Gaussian function with $s_d=0.1m$ and aspect ratio $H/(4s_d)=0.1$. Figure 3.a corresponds to $u_{*0}=0.04$ m/s, Fig 3.b corresponds to $u_{*0}=0.08$ m/s, Fig. 3.c corresponds to $u_{*0}=0.16$ m/s and all the other parameters are the same as in Fig. 1.

From Fig. 3b we observe that, due to the increased relaxation effect (increased phase shift between q and q_{sat}) the growth rate is smaller when $C_{sat}=50$ in comparison with $C_{sat}=1$ (Fig. 1.b). From Fig. 3.c, the relaxation effects are even larger, being stronger than the unstable mechanism and being responsible for the stabilization of the bed. As the phase shift between q and q_{sat} varies with the shear velocity of the basic flow (Eq. 6), the combination $u_{*0}=0.16$ m/s and $C_{sat}=50$ induces a shift between q and the bed morphology downstream to the crest of the bed, as shown in Fig. 2.c. This corresponds to a stable situation. The increasing of the relaxation effect also occurs in Fig. 3.a, however the time-scale is too large (slow growth rate) to be clear in the figure.

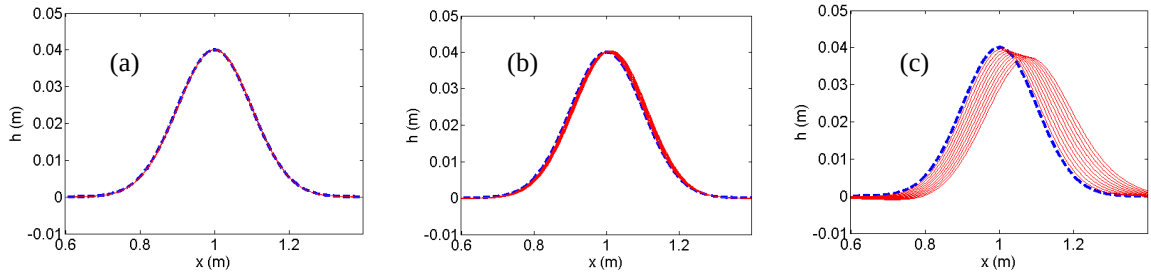

Figure 3. Evolution of an initial gaussian bedform, with $s_d=0.1m$ and aspect ratio $H/(4s_d)=0.1$. The dashed line is the initial form and the continuous lines correspond to the bedform at posterior times. The total time for this simulation was 1 s. The saturation adjustable constant is $C_{sat}=50$. (a) corresponds to $u_{*0}=0.04$ m/s, (b) corresponds to $u_{*0}=0.08$ m/s and (c) corresponds to $u_{*0}=0.16$ m/s.

It is important to comment here about the apparent differences between the results of the presented simulations and the stability analysis of Franklin (2010). In Franklin (2010), a stability analysis was made on a continuum spectrum of modes, and the most unstable one (most amplified growth rate) was found for a given wavelength. Predictions of the variations of the growth rate and of the celerity were then made for this specific wavelength. Also, Franklin (2010) showed the existence of a cut-off wavelength, below which the bed is always stable.

In the present work, the initial bedform is imposed as an initial condition in the simulations and, from that, its evolution is computed in the early stages of the instability (or stability). In this case, for an initial length $L = 4\ s_d = 0.4m$, values of the adjustable constant $C_{sat}=1$ or $C_{sat}=10$ are too small for the phase shift between the bed-load flow rate and the fluid flow to influence the growth rate and the celerity. To find the growth rate and the celerity variations predicted by the stability analysis of Franklin (2010), it is necessary to increase the values of C_{sat}. Other way to obtain these variations would be to change the length of the initial bedform. In other words, the numerical code, different from the stability analysis, does not select the most unstable mode. Comparisons between the code and the stability analysis can be made by computing numerically the evolution of the bedform when employing the most unstable mode as the initial bedform.

The presented numerical code is expected to give results in accordance with Franklin (2010) if the initial bedform correspond to the wavelength of the most unstable mode. Also, by varying the length of the initial bedform, the cut-off wavelength shall appear in the simulations as that below which the growth rate is negative. Simulations of this kind are left for a future work.

5. CONCLUSION

This communication presented a mathematical model for the bed-load transport by a turbulent boundary-layer, when the fluid is a liquid. The model was kept as simple as possible, and is valid whenever the aspect ratio of the initial form is less than *0.3*. The model was implemented in a numerical code and some simulations were presented.

The numerical simulations showed that the model captures the pertinent physics involved, such as the growing of instabilities on the bed surface. Given an initial gaussian bedform, of low aspect ratio, the simulations showed its increase, tending to a ripple form (as observed in nature and in experiments), or its decrease, tending to a flat bed.

The numerical results were confronted to the stability theory of Franklin (2010), in the case of variations of the fluid flow (shear velocity) of the basic state. The comparisons were not straight because the stability analysis was done in a continuum spectrum of modes, predicting growth rates and celerities for the most unstable mode. In the presented numerical code, the evolution was computed in the early stages of the instability (or stability) for an imposed initial bedform.

The presented numerical code is expected to give results in accordance with Franklin (2010) if the initial bedform correspond to the wavelength of the most unstable mode. Also, by varying the length of the initial bedform, the cut-off wavelength shall appear in the simulations as that below which the growth rate is negative. Simulations of this kind are left for a future work.

6. ACKNOWLEDGEMENTS

The author is grateful to grateful to Petrobras S.A. for the financial support (contract number 0050.0045763.08.4).

7. REFERENCES

Bagnold, R.A., 1941, “The physics of blown sand and desert dunes”, Ed. Chapman and Hall, London, United Kingdom, 320 p.

Buffington, J.M. and Montgomery, D.R., 1997, “A systematic analysis of eight decades of incipient motion studies, with special reference to gravel-bedded rivers”, Water Resour. Res., Vol.33, pp. 1993-2029.

Carruthers, D.J. and Hunt, J.C.R., 1990, “Fluid mechanics of airflows over hills: turbulence, fluxes, and waves in the boundary layer”, Atmospheric Processes over Complex Terrain, Vol.23, pp. 83-108.

Clift, R., Grace, J. and Weber, M., 1978, “Bubbles, drops and particles”, Ed. Dover Publications, Inc., New York, United States of America, 400p.

Charru, F., Mouilleron-Arnould, H. and Eiff, O., 2004, “Erosion and deposition of particles on a bed sheared by a viscous flow”, J. Fluid Mech., Vol. 519 pp. 55 - 80.

Charru, F., 2006, “Selection of the ripple length on a granular bed sheared by a liquid flow”, Physics of Fluids, Vol. 18 (121508).

Charru, F., 2007, “Instabilités hydrodynamiques”, Ed. EDP Sciences, Les Ulis, France, 386 p.

Claudin, P. and Andreotti, B., 2006, “A scaling law for aeolian dunes on Mars, Venus, Earth, and for subaqueous ripples”, Earth Plan. Sci. Lett., Vol. 252, pp. 20 - 44.

Drazin, P.G. and Reid, W.R., 2004, “Hydrodynamic stability”, Ed. Cambridge University Press, Cambridge, United Kingdom, 605 p.

Elbelrhiti, H., Claudin, P. and Andreotti, B., 2005, "Field evidence for surface-waveinduced instability of sand dunes", Nature Vol. 437 (04058).
Engelund, F., 1970, "Instability of erodible beds", J. Fluid Mech., Vol. 42, pp. 225 - 244.
Engelund, F. and Fredsoe, J., 1982, "Sediment ripples and dunes", Ann. Rev. Fluid Mech., Vol. 14, pp. 13 - 37.
Franklin, E.M., 2010, "Initial instabilities of a granular bed sheared by a turbulent liquid flow: length-scale determination", J. Braz. Soc. Mech. Sci. Eng., Vol. 32, pp. 460-467.
Franklin, E.M., 2011, "Non-linear instabilities on a granular bed sheared by a turbulent liquid flow", J. Braz. Soc. Mech. Sci. Eng., accepted.
Franklin, E.M., 2008, "Dynamique de dunes isolées dans un écoulement cisaillé", (in french), Ph.D. Thesis, Université de Toulouse, Toulouse, France, 166 p.
Hersen, P., 2004, "On the crescentic shape of barcahn dunes", Eur. Phys. J. B, Vol.4, pp. 507-514.
Hunt, J. C. R., Leibovich, S. and Richards, K., 1988, "Turbulent shear flows over low Hills", Quart. J. R. Met. Soc., Vol. 114, pp. 1435 - 1470.
Jackson, P.S. and Hunt, J. C. R., 1975, " Turbulent wind flow over a low hill", Quart. J. R. Met. Soc., Vol. 101, pp. 929 - 955.
Kennedy, J. F., 1963, "The mechanics of dunes and antidunes in erodible-bed channels", J. Fluid Mech., Vol. 16, pp. 521 - 544.
Kroy, K., Sauermann, G. and Herrmann, H.J., 2002a, "Minimal model for sand dunes", Phys. Rev. Letters, Vol. 88 (054301).
Kroy, K., Sauermann, G. and Herrmann, H.J., 2002b, "Minimal model for aeolian sand dunes", Phys. Rev. E, Vol. 66 (031302).
Kuru, W. C., Leighton, D. T. and McCready M. J., 1995, "Formation of waves on a horizontal erodible bed of particles", Int. J. Multiphase Flow, Vol. 21, No.6, pp. 1123 -1140.
Landau, L.D. and Lifchitz, E.M., 1994, "Physique théorique: mécanique des fluides", Ed. Ellipses (traduction française), Poitiers, France, 752 p.
Meyer-Peter, E. and Mueller, R., 1948, "Formulas for bed-load transport", Proceedings of the 2nd Meeting of the International Association for Hydraulic Research, Stokholm, Sweden.
Raudkivi, A.J., 1976, "Loose boundary hydraulics", Ed. Pergamon, Oxford, United Kingdom, 397p.
Reynolds, A.J., 1964, "Waves on the erodible bed of an open channel", J. Fluid Mech., Vol. 22 pp. 113 - 133.
Richards, K.J., 1980, "The formation of ripples and dunes on an erodible bed", J. Fluid Mech., Vol. 99, pp. 597 – 618
Sauermann, G., Kroy, K. and Herrmann, H.J., 2001, "A continuum saltation model for sand dunes", Phys. Rev. E, Vol. 64 (31305).
Schmid, P.J. and Henningson, D.S., 2001, "Stability and transition in shear flows", Ed. Springer, New York, United States of America, 556 p.
Valance, A. and Langlois, V., 2005, "Ripple formation over a sand bed submitted to a laminar shear flow", Eur. Phys. J. B, Vol. 43, pp. 283 - 294.
Weng, W. S., Hunt, J. C. R., Carruthers, D. J. , Warren, A., Wiggs, G. F. S., Livingstone, I. , and Castro, I., 1991, "Air flow and sand transport over sand-dunes", Acta Mechanica, pp. 1 – 21.

8. RESPONSIBILITY NOTICE

The author is the only responsible for the printed material included in this paper.